Can OSiS Be Formed in the Interstellar Medium? A Computational Investigation of the OH + SiS Reaction with a Kinetic Analysis

Nadia Balucani[1(✉)], Luca Mancini[1], Dimitrios Skouteris[2], Cecilia Ceccarelli[3], Linda Podio[4], Claudio Codella[4], Gabriella Di Genova[1], and Marzio Rosi[5]

[1] Dipartimento di Chimica, Biologia e Biotecnologie, Università degli Studi di Perugia, 06123 Perugia, Italy
{nadia.balucani,luca.mancini}@unipg.it
[2] Master-Tec SrL, Via Gerardo Dottori, 94, 06132 Perugia, Italy
[3] Université Grenoble Alpes, CNRS, IPAG, 38000 Grenoble, France
[4] INAF, Osservatorio Astrofisico di Arcetri, Largo E. Fermi 5, 50125 Florence, Italy
[5] Dipartimento di Ingegneria Civile ed Ambientale, Università degli Studi di Perugia, 06125 Perugia, Italy
marzio.rosi@unipg.it

Abstract. A few years ago, silicon oxysulfide, OSiS, was suggested as a possible interstellar molecule containing both sulfur and silicon. Its detection using remote spectroscopy has so far been unsuccessful, and only upper limits have been reported in the literature. It remains to be seen whether efficient formation pathways exist that warrant further search. An initial suggestion for the OSiS formation indicated the O + SiS reaction, but this cannot form OSiS under the rarefied conditions of the interstellar medium, since stabilizing secondary or three-body collisions are highly unlikely. For this reason, following the example of reactions such as OH + CO, OH + CS, and OH + SiO we report a computational investigation of the OH + SiS reaction. According to our electronic structure calculations, which allowed us to construct the potential energy surface of the reactive system, the OH + SiS reaction can lead to the formation of OSiS + H, but a much more competitive pathway leads to SiO + HS. Our preliminary kinetic analysis showed that the yield of OSiS + H is ca. 17% at the temperatures of interest for the interstellar medium. Our results will be compared with those of a recent similar study, and the astrophysical implications will be noted.

Keywords: Electronic structure calculations · Kinetic calculations · Astrochemistry · Silicon chemistry

1 Introduction

Interstellar chemistry plays a fundamental role in the matter evolution within a galaxy, linking stellar nucleosynthesis to solar-system formation. Silicon and sulfur are both alpha process elements [1] and are among the most abundant elements of the third

© The Author(s), under exclusive license to Springer Nature Switzerland AG 2027
O. Gervasi et al. (Eds.): ICCSA 2026 Workshops, LNCS 16760, pp. 453–465, 2027.
https://doi.org/10.1007/978-3-032-30521-3_29

period of the Periodic Table [2]. They are both believed to become part of refractory materials when the density is high and the temperature is low [3]. However, while there is little doubt that silicon is mostly retained as silicates in the core of interstellar dust grains [4], the main reservoir of interstellar sulfur is still debated [5]. In recent years, considerable effort has been made to characterize the abundance of gaseous S-bearing species (see, for instance, [5–8]) and the possible inventory of S-molecules on ice (only $OCS_{(ice)}$ has been detected so far [9], and possibly $SO_{2(ice)}$ [10]). As of today, the puzzle of sulfur depletion in cold clouds and star-forming regions is far from being solved [5].

Silicon is heavily depleted onto dust grains under quiescent conditions. Therefore, the presence of its molecules in the gas phase is considered an important tracer of shock-driven chemistry, as energetic processes are required to release refractory elements from dust grains. Molecules containing both sulfur and silicon, such as silicon sulfide (SiS), may offer insights into the long-standing problem of sulfur depletion in dense clouds since both S and Si are released in the gas phase by shocks and outflows [11]. Numerous formation routes of SiS have been considered, including neutral-neutral reactions [12–17] and ion-molecule reactions [18,19]. In addition to SiS, silicon oxysulfide, OSiS, has been proposed as another possible interstellar molecule where both sulfur and silicon are present [20]. After its isolation and characterization in a cold-matrix experiment [21], the rotational spectroscopy of OSiS was characterized in the gas phase [22], and its astronomical search has been pursued to date without success [23].

Even before confirming its presence (only upper limits are available in the literature [23]), the possible formation routes of OSiS have been analyzed. In shocked regions, SiS is normally present, and therefore, the formation pathways of OSiS could start from SiS. An initial study considered the O + SiS reaction [20], but it cannot work in the rarefied conditions of the interstellar medium because stabilizing secondary or three-body collisions are highly improbable. Considering the analogous reactions OH + CO → CO_2 + H [24], OH + SiO → SiO_2 + H [25], and OH + CS → OCS + H [26], the OH + SiS reaction, which is the subject of this study, emerges as a possible formation route of OSiS. This reaction was considered by Costa et al. [27] very recently, together with other silicon reactions. They characterized the OH + SiS potential energy surface (PES) at the CCSD(T)-F12/cc-pVQZF12//M06-2X/aug-cc-pV(T+d)Z + ZPE(M06-2X/aug-ccpV(T+d)Z) level of theory.

Here, we present our calculations obtained at the CCSD(T)/CBS//ωB97XD/aug-cc-pV(T+d)Z) level of theory. In addition to deriving a more complete PES, in which additional pathways are present, we have also performed Rice-Ramsperger-Kassel-Marcus (RRKM) calculations to estimate the product branching fractions of the two open channels

$$\mathrm{OH} + \mathrm{SiS} \longrightarrow \mathrm{HS} + \mathrm{SiO} \tag{1}$$

$$\mathrm{OH} + \mathrm{SiS} \longrightarrow \mathrm{OSiS} + \mathrm{H}. \tag{2}$$

The computed branching fraction of reaction (2) is smaller than the value estimated by Costa et al. [27] without performing a kinetic analysis of the PES.

2 Theoretical Methods

The OH + SiS reaction was characterized by adopting the same computational strategy already used for other bimolecular reactions (see, for instance, [12,28–35]) and using the GAUSSIAN09 [36] and Molpro [37] software packages. All stationary points were first optimized at the DFT ωB97XD level of theory [38], in conjunction with the correlation consistent valence polarised set aug-cc-pV(T+d)Z [39–41]. Harmonic vibrational frequencies were computed, at the same level of theory, to determine the nature of each stationary point, that is, a minimum (reactants, reaction intermediates and products) if all the frequencies are real, and a first-order saddle point (transition state) if there is one, and only one, imaginary frequency. When a saddle point was found, Intrinsic Reaction Coordinate (IRC) calculations [42,43] were performed to assign each transition state to the respective reactant and product. After each geometry optimization at the DFT level, more accurate calculations were performed using the single- and double-electronic excitation coupled-cluster method with perturbative description of triple excitations, CCSD(T) [44–46], corrected with a Density Fitted (DF)MP2 extrapolation to the complete basis set (CBS) and with corrections for core electron excitations. Namely, the energy values were computed according to:

$$E(\text{CCSD(T)/aug-cc-pVTZ}) + E(1) + E(2) \tag{3}$$

where

$$E(1) = E(\text{CCSD(T,core)/cc-pVTZ}) - E(\text{CCSD(T)/cc-pVTZ})$$
$$E(2) = E(\text{DF-MP2/CBS}) - E(\text{DF-MP2/aug-cc-pVTZ})$$

with E(DF-MP2/CBS) defined as:

$$\begin{aligned} E(\text{DF-MP2/CBS}) = {} & E[(\text{DF-MP2})/\text{aug-cc-pVQZ})] \\ & + 0.5772 * [E(\text{DF-MP2/aug-cc-pVQZ}) \\ & - E(\text{DF-MP2/aug-cc-pVTZ})] \end{aligned} \tag{4}$$

The E(DF-MP2/CBS) extrapolation was performed using Martin's two-parameter scheme [47], leading to an expected accuracy of about ± 5 kJ mol^{-1}. These energies, labeled CBS despite also including core-valence correlation corrections, were used for the kinetic investigation described below. The zero-point-energy (ZPE), evaluated at the DFT level of theory, was used to correct all energy values. Given the uncertainty in the calculations, all reported energy values have been rounded to the nearest integer. In a few cases, an additional decimal place is provided to indicate the relative ordering of structures with very similar energies.

The branching fraction of the products has been calculated by employing a combination of RRKM and master-equation programs developed by us and previously described in detail [48–50].

3 Results

The complete PES is reported in Fig. 1, while the structures of the reactants, products, intermediates, and transition states are shown in Figs. 2, 3, and 4. The energy values

of the stationary points obtained at the two employed levels of theory are shown in Fig. 1 (black: DFT ωB97XD level of theory; in blue and in brackets the data obtained at the CBS level) and reported in Table 1. To evaluate the possible multireference character of the investigated sulfur-containing systems, T1 diagnostics were computed for the relevant stationary points [51]. The obtained values (ca. 0.02, consistently below the accepted threshold of 0.03) indicate that multireference effects are limited, supporting the suitability of the present approach for reliably describing the present potential energy surfaces.

The reaction starts with the addition of OH to SiS, either on the S or Si side.

When adding to the Si side, the addition intermediate MIN1, quite stable with respect to the reactants (−284 kJ/mol at the CBS level of theory), is formed. Once formed, MIN1 can dissociate directly via the O-H bond fission and form OSiS + H. However, to do that, TS2 (a very high-energy transition state, +254 kJ/mol) must be overcome, making this direct channel quite improbable. Instead, MIN1 can easily isomerize into MIN2c by overcoming a much lower transition state (TS1, located at −121 kJ/mol) or into MIN3 by overcoming TS5 (−102 kJ/mol). Once formed, MIN2c can, in turn, easily isomerize to its *trans* isomer MIN2t (via TS7 located at −204 kJ/mol) or dissociate into SiO + SH (a channel without an exit barrier) or into OSiS + H; in this case, an energy barrier associated with TS3 (−45 kJ/mol) must be overcome. Also MIN2t can dissociate into SiO + SH via a barrierless exit channel or into OSiS + H by overcoming an exit barrier associated with TS8 (−43 kJ/mol). Given the very similar geometries and energies, TS3 and TS8 may be regarded as conformationally related transition structures associated with distinct cis/trans intermediates. MIN3 can only isomerize back to MIN1 or dissociate into OSiS + H by passing through the critical configuration of TS6. This transition state is located at −40 kJ/mol at the DFT ωB97XD level of theory (and in this case it is an exit barrier toward the products OSiS + H, whose energy content is −43 kJ/mol) or at −57 kJ/mol at the CBS level of theory. In this second case, TS6 exhibits the characteristics of a submerged transition state along the route toward the OSiS + H product (characterized by an energy content of −55 kJ/mol at the same level of theory).

When adding to the S side, the MIN4c intermediate is formed, associated with a swallow minimum (−43 kJ/mol at the CBS level). MIN4c can easily isomerize to its *trans* isomer MIN4t (−41 kJ/mol at the CBS level) via TS9. MIN4t can isomerize to MIN1 by overcoming a barrier associated with TS4 located at −5 kJ/mol relative to the reactants. Therefore, TS4 is a submerged transition state at this level of theory. Given the uncertainty in the current calculations, TS could also be at the same energy level as, or slightly above, that of the reactants.

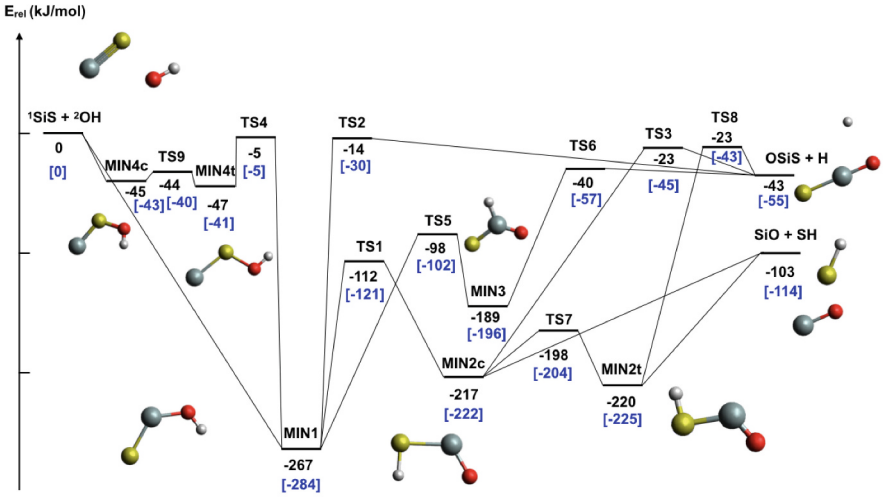

Fig. 1. Schematic representation of the potential energy surface obtained for the OH + SiS reaction at the CCSD(T)/CBS//ωB97XD/aug-cc-pV(T+d)Z) level of theory. Sulfur atoms are shown in yellow, silicon in gray, oxygen in red, and hydrogen in white. (Color figure online)

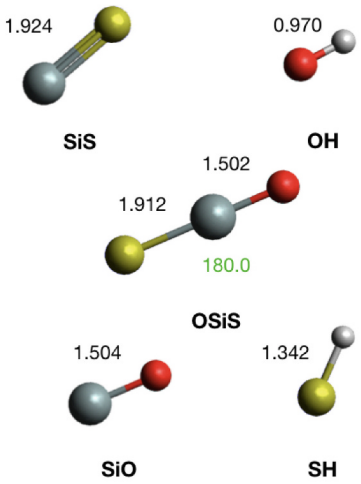

Fig. 2. ωB97XD optimized geometries (Å and deg) of the reactants and products. Sulfur atoms are shown in yellow, silicon in gray, oxygen in red, and hydrogen in white. (Color figure online)

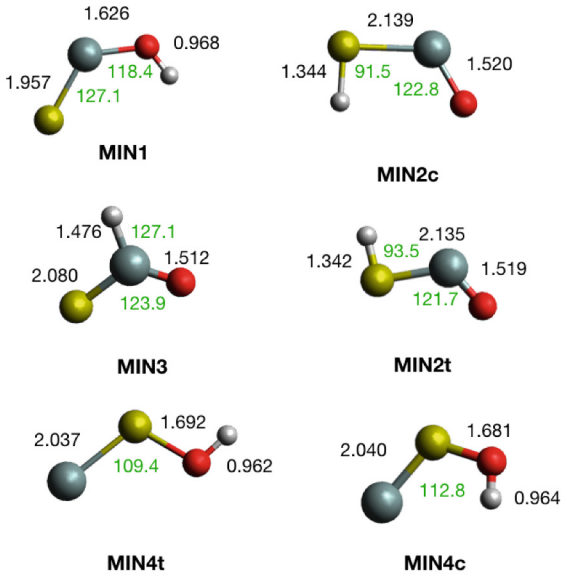

Fig. 3. ωB97XD optimized geometries (Å and deg) of the intermediates formed during the reaction OH + SiS (see Fig. 1). Sulfur atoms are shown in yellow, silicon in gray, oxygen in red, and hydrogen in white.

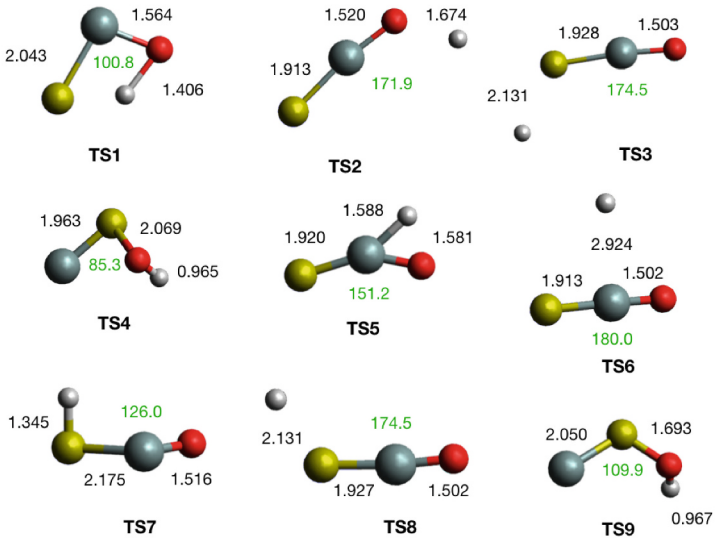

Fig. 4. ωB97XD optimized geometries (Å and deg) of the transition states characterizing the OH + SiS PES (see Fig. 1). Sulfur atoms are shown in yellow, silicon in gray, oxygen in red, and hydrogen in white.

Our PES scheme has many similarities to the one derived by Costa et al. [27], but also a few differences. For example, the MIN4 intermediates cannot evolve along their PES, whereas in our case they isomerize to MIN1 by overcoming a submerged barrier (TS4). Table 1 reports the energy values of the stationary points of the PES calculated in this work at the ωB97XD/aug-cc-pV(T+d)Z and CCSD(T)/CBS//ωB97XD/aug-cc-pV(T+d)Z) level of theory to be compared with those reported by Costa et al., obtained at the CCSD(T)-F12/cc-pVQZF12//M06-2X/aug-cc-pV(T+d)Z level of theory. In many cases, the small differences found between our CBS calculations and theirs are within the uncertainty of the methods used.

The most significant differences in the two PESs is actually related to the reverse reaction H + OSiS. Indeed, in our PES there is a significant exit barrier along the possible pathways leading to OSiS + H, see the sequences MIN1 → TS2 → OSiS+H, MIN2c → TS3 → OSiS+H, MIN2t → TS8 → OSiS+H. The structures of the involved TS are shown in Fig. 4. The only pathway in which the TS associated with the formation of the products is submerged is MIN3 → TS6 → OSiS+H. According to the calculations by Costa et al., instead, the pathways i3 → OSiS+H (equivalent to our MIN3 → TS6 → OSiS+H) and i4 → OSiS+H (equivalent to our MIN2t → TS8 → OSiS+H) are barrierless. In the case of MIN3 → TS6 → OSiS+H, the energy of TS6 is −40 kJ/mol at the ωB97XD/aug-cc-pV(T+d)Z level to be compared with ΔH_0^o(OSiS + H) of −43 kJ/mol but, if we consider the CBS higher level of calculations, TS6 is a submerged transition state having an energy of −57 kJ/mol to be compared with ΔH_0^o(OSiS + H) of −55 kJ/mol. In other words, while our work excludes that the other H attacks on OSiS are barrierless, in this specific case, the formation of MIN3 from the H + OSiS reaction could also occur under cold-cloud conditions in the interstellar medium. Since hydrogen atoms are ubiquitous in the interstellar medium, the fact that the reaction can occur without a barrier in the entrance channel is extremely relevant to determine the resistance of OSiS, since the reaction with H would very easily destroy it. A similar condition had already been discussed for the H + SiS_2 reaction [12,49]: the lack of a barrier in the entrance channel makes the reaction extremely fast, systematically converting interstellar SiS_2 (that can be formed by the SiH + S_2 reaction) into SiS+HS. Remarkably, also the H + SiO_2 reaction is not characterized by an entrance barrier. However, in that case, there are no open exothermic channels and SiO_2, once formed, cannot be destroyed by the H atoms (see the Discussion in [49]). To be noted that also in the case of H + SiO_2 and H + SiS_2 it is the formation of trigonal structures with the Si engaged in three bonds that can be formed without an activation energy, while the H addition to one of the O atoms of SiO_2 or one of the S atoms of SiS_2 is always associated with an entrance barrier. This result is somewhat surprising because of the available lone pairs on O and S atoms. Furthermore, the addition of H to the central Si atom of OSiS, SiS_2, and SiO_2 requires a hybridization change of the central Si atom from sp to sp^2. Clearly, the new Si-H bond is strong enough to compensate for the significant change required in the molecular backbone.

3.1 The Product Branching Fraction

Since this calculation serves only to establish the branching fraction between the two channels (1) and (2), we did not conduct a complete kinetic analysis of the PES

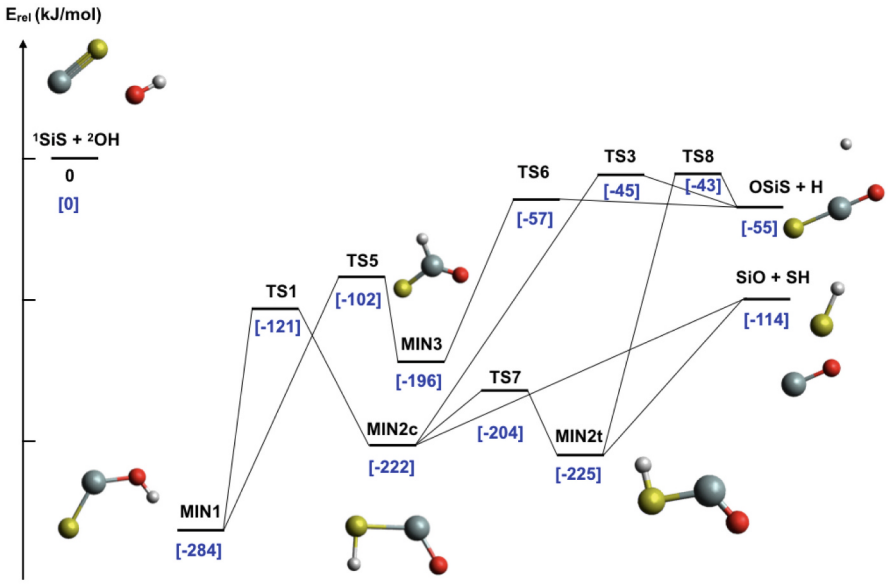

Fig. 5. Portion of the potential energy surface illustrated in Fig. 1 that has been used to evaluate the product branching fractions via RRKM calculations. Sulfur atoms are shown in yellow, silicon in gray, oxygen in red, and hydrogen in white.

(deferred to more comprehensive future work). We started from MIN1 and considered only the pathways originating after its isomerization to MIN2c and MIN3, i.e., we have analyzed only the reduced portion of the PES shown in Fig. 5. After solving the master equation for the paths illustrated in Fig. 5 and averaging the microcanonical constants over the Boltzmann distribution, we calculated the BFs at the most interesting temperatures in the interstellar medium, namely 10, 100, and 200 K (see Table 2). We also calculated the value at room temperature. In line with the characteristics of the PES, the SiO + HS formation channel is by far the dominant one and there is a little trend with the temperature with the yield of OSiS + H iscreasing from 16.6% to 18.4%. Therefore, the yield of OSiS is lower than the 25% yield suggested by Costa et al., who assumed this value at all temperatures considered.

Table 1. Energies (kJ/mol, 0 K) of the stationary points of the OH + SiS PES, computed at the indicated level of theory (present work: ωB97XD/aug-cc-pV(T+d)Z and CCSD(T)/CBSωB97XD/aug-cc-pV(T+d)Z) level of theory; Costa et al. [27]: CCSD(T)-F12/cc-pVQZF12//M06-2X/aug-cc-pV(T+d)Z level of theory).

	ωB97XD/aug-cc-pV(T+d)Z this work	CBS this work	CCSD(T)- F12/cc-pVQZF12// M06-2X/aug-cc-pV(T+d)Z [27]
MIN1	−267	−284	−281 (i2c in [27])
MIN2(cis)	−217	−222	−218
MIN2(trans)	−220	−225	−222 (i4t in [27])
MIN3	−189	−196	−190 (i3 in [27])
MIN4(cis)	−45	−43	−39 (i1c in [27])
MIN4(trans)	−47	−41	−37
TS1	−112	−121	−117
TS2	−14	−30	−30
TS3	−23	−45	/
TS4	−5	−5	/
TS5	−98	−102	−98
TS6	−40	−57	/
TS7	−198	−204	/
TS8	−23	−43	/
TS9	−44	−40	/
ΔH_0^o(SiO + SH)	−103	−114	−110
ΔH_0^o(OSiS + H)	−43	−55	−54

4 Discussion and Astrophysical Implications

In this work, we addressed the theoretical study of the OH + SiS reaction as a possible mechanism for the formation of OSiS in shocked regions of the interstellar medium. Based on other similar reactions, particularly OH + CS, OH + SiO, and OH + CO, it was reasonable to expect the formation of OSiS. However, potential energy surface analysis immediately shows that the reaction channel leading to OSiS + H is strongly disfavored compared to the more exothermic SiO + HS channel. Kinetic analysis using the RRKM method confirmed a lower yield of channel (2) (<18% under conditions typical of star-forming regions). Therefore, the value suggested by Costa et al. [27] overestimates the yield of channel (2).

Furthermore, the previous conclusions by Costa et al. [27] on the destruction of OSiS by atomic hydrogen require further investigation. It is unclear whether or not an activation energy exists for the reaction H + OSiS → SiO + HS. However, even if TS6 is confirmed to be submerged relative to H + OSiS, its presence still represents a bottleneck for the reactive flux. Since there is certainly a van der Waals complex between the reactants and TS6, the combination of the two will increase back-dissociation. Therefore, a gas kinetic rate constant such as the one suggested by Costa et al. (4×10^{-10}

Table 2. Product branching fractions at different temperatures of relevance to the chemistry of the interstellar medium. Calculations were performed using the RRKM method, taking into account the paths originating from the MIN2 intermediate, as these are the minimum energy paths for the formation of both the SiO + HS and OSiS + H products (see the scheme reported in Fig. 5).

channel	T = 10 K	T = 100 K	T = 200 K	T = 300 K
SiO + SH	83.4%	83.0%	82.1%	81.6%
OSiS + H	16.6%	17.0%	17.9%	18.4%

$cm^3\ mol^{-1}$) seems to be implausible. Clearly, the most important role of the OH + SiS reaction is to convert SiS to SiO as already observed in the reaction O + SiS [14].

5 Conclusions

This study represents another piece in the puzzle of SiS chemistry. There are many reasons to try to understand the genesis of this molecule in the interstellar medium and also in the circumstellar envelopes of asymptotic giant branch and red supergiants stars. Its relationship with the similar molecule SiO is not only linked to the larger abundance of oxygen compared to sulfur. Since both silicon and sulfur are strongly depleted in the dense regions of the interstellar medium, they are released together into the gas phase due to shock waves. SiO and SiS probably form at different times, and their fate, once formed, is also different. An excess of oxygen species systematically converts SiS to SiO. This was already known for the O + SiS reaction and is now also known for the OH + SiS reaction. The formation of OSiS by reactions involving SiS does not seem to contribute to preserving the Si-S bond because they are too uncompetitive with other reaction channels that convert SiS to SiO. There are still many aspects to be clarified and which require dedicated studies such as the one shown here.

Acknowledgments. The authors thank the Italian MUR PRIN2020 (2020AFB3FX - Astrochemistry beyond the second period elements). MR and LP acknowledge financial support under the National Recovery and Resilience Plan (NRRP), Mission 4, Component 2, Investment 1.1, Call for tender No. 104 published on 2.2.2022 by the Italian Ministry of University and Research (MUR), funded by the European Union – NextGenerationEU– Project Title 2022JC2Y93 ChemicalOrigins: linking the fossil composition of the Solar System with the chemistry of protoplanetary disks – CUP J53D23001600006 - Grant Assignment Decree No. 962 adopted on 30.06.2023 by the Italian Ministry of Ministry of University and Research (MUR).

Disclosure of Interests. The authors have no competing interests to declare that are relevant to the content of this article.

References

1. Goswami, S., Vilchez, J.M., Pérez-Díaz, B., Silva, L., Bressan, A., Pérez-Montero, E.: Contribution of very massive stars to the sulfur abundance in star-forming galaxies: role of pair-instability supernovae. A&A **685**, A81 (2024). https://doi.org/10.1051/0004-6361/202348231
2. Asplund, M., Grevesse, N., Sauval, A.J., Scott, P.: The chemical composition of the sun **47**(1), 481–522 (2009). https://doi.org/10.1146/annurev.astro.46.060407.145222
3. Jenkins, E.B.: A unified representation of gas-phase element depletions in the interstellar medium. Astrophys. J. **700**(2), 1299 (2009). https://doi.org/10.1088/0004-637X/700/2/1299
4. Draine, B.T.: Interstellar dust grains, vol. 41, pp. 241–289 (2003). https://doi.org/10.1146/annurev.astro.41.011802.094840
5. Laas, J.C., Caselli, P.: Modeling sulfur depletion in interstellar clouds. A&A **624**, A108 (2019). https://doi.org/10.1051/0004-6361/201834446
6. Fuente, A., et al.: Gas phase elemental abundances in molecular clouds (GEMS) - VII. sulfur elemental abundance. A&A **670**, A114 (2023). https://doi.org/10.1051/0004-6361/202244843
7. Rivière-Marichalar, P., et al.: Observations of sulfuretted species in HL Tau. A&A **703**, A282 (2025)
8. Taquet, V., et al.: Seeds of life in space (SOLIS) - VI. Chemical evolution of sulfuretted species along the outflows driven by the low-mass protostellar binary NGC 1333-IRAS4A. A&A **637**, A63 (2020). https://doi.org/10.1051/0004-6361/201937072
9. Palumbo, M., Geballe, T., Tielens, A.G.: Solid carbonyl sulfide (OCS) in dense molecular clouds. Astrophys. J. **479**(2), 839–844 (1997)
10. Gross, R.E., et al.: CORINOS. IV. Quantifying Baseline-fitting Uncertainties in SO_2 ice measurements with JWST/MIRI **998**(1), 68 (2026). https://doi.org/10.3847/1538-4357/ae2c81
11. Podio, L., et al.: Silicon-bearing molecules in the shock L1157–B1: first detection of SiS around a Sun-like protostar. Mon. Not. Roy. Astron. Soc. Lett. **470**(1), L16–L20 (2017)
12. Rosi, M., et al.: Possible scenarios for SiS formation in the interstellar medium: electronic structure calculations of the potential energy surfaces for the reactions of the SiH radical with atomic sulphur and S_2. Chem. Phys. Lett. **695**, 87–93 (2018)
13. Rosi, M., et al.: Electronic structure and kinetics calculations for the Si+SH reaction, a possible route of SiS formation in star-forming regions. In: Misra, S., et al. (eds.) ICCSA 2019. LNCS, vol. 11621, pp. 306–315. Springer, Cham (2019). https://doi.org/10.1007/978-3-030-24302-9_22
14. Zanchet, A., Roncero, O., Agundez, M., Cernicharo, J.: Formation and destruction of SiS in space. ApJ **862**(1), 38 (2018). https://doi.org/10.3847/1538-4357/aaccff
15. Mota, V.C., Caridade, P.J.S.B., Varandas, A.J.C., Galvao, B.R.L.: Quasiclassical trajectory study of the Si plus SH reaction on an accurate double many-body expansion potential energy surface. J. Phys. Chem. A **126**(22), 3555–3568 (2022). https://doi.org/10.1021/acs.jpca.2c01633
16. Doddipatla, S., He, C., Goettl, S.J., Kaiser, R.I., Galvão, B.R., Millar, T.J.: Nonadiabatic reaction dynamics to silicon monosulfide (SiS): a key molecular building block to sulfur-rich interstellar grains. Sci. Adv. **7**(26), eabg7003 (2021)
17. Fortenberry, R.C., McGuire, B.A.: A possible additional formation pathway for the interstellar diatomic SiS. Astroph. J. **971**(1), 101 (2024). https://doi.org/10.3847/1538-4357/ad4d94
18. Michielan, M., et al.: Experimental and computational investigation of an ionic pathway to the formation of silicon sulphide in the interstellar medium. A&A **698**, A205 (2025)

19. Mancini, L., Trinari, M., de Aragão, E.V.F., Rosi, M., Balucani, N.: The $S^+(^4S)$+ SiH_2 ($^1A_1$) reaction: toward the synthesis of interstellar SiS. In: International Conference on Computational Science and Its Applications, pp. 233–245. Springer (2022). https://doi.org/10.1007/978-3-031-10562-3_17
20. Paiva, M.A.M., Lefloch, B., Galvão, B.R.L.: Accurate theoretical predictions on the mechanisms of OSiS formation and its dissociation channels. Mon. Not. Roy. Astron. Soc. **481**(2), 1858–1861 (2018). https://doi.org/10.1093/mnras/sty2382
21. Schnöckel, H.: Matrix isolation of OSiS: IR spectroscopic evidence for the sis double bond. Angew. Chem. Int. Ed. Engl. **19**(4), 323–324 (1980). https://doi.org/10.1002/anie.198003231
22. Thorwirth, S., Mück, L.A., Gauss, J., Tamassia, F., Lattanzi, V., McCarthy, M.C.: Silicon Oxysulfide, OSiS: rotational spectrum, quantum-chemical calculations, and equilibrium structure. J. Phys. Chem. Lett. **2**(11), 1228–1231 (2011). https://doi.org/10.1021/jz200368x
23. Esplugues, G.B., et al.: A line confusion-limited millimeter survey of Orion KL - III. Sulfur oxide species. A&A **556**, A143 (2013). https://doi.org/10.1051/0004-6361/201321285
24. Caracciolo, A., et al.: Combined experimental–theoretical study of the OH + CO → H + CO_2 reaction dynamics. J. Phys. Chem. Lett. **9**(6), 1229–1236 (2018). https://doi.org/10.1021/acs.jpclett.7b03439
25. Martín, J.C.G., Blitz, M.A., Plane, J.M.: Kinetic studies of atmospherically relevant silicon chemistry. Part II: Silicon monoxide reactions. Phys. Chem. Chem. Phys. **11**(46), 10945–10954 (2009)
26. Adriaens, D., Goumans, T., Catlow, C., Brown, W.: Computational study of carbonyl sulphide formation on model interstellar dust grains. J. Phys. Chem. C **114**(4), 1892–1900 (2010)
27. Costa, S.F., Alves, M.O., Pilling, S., Li, J., Galvão, B.R.: New neutral-neutral pathways in the chemistry of silicon-and sulfur-bearing molecules in the cold interstellar medium. Astrophys. J. **995**(2), 209 (2025)
28. Skouteris, D., Balucani, N., Faginas-Lago, N., Falcinelli, S., Rosi, M.: Dimerization of methanimine and its charged species in the atmosphere of Titan and interstellar/cometary ice analogs. Astron. Astrophys. **584**, A76 (2015)
29. Giani, L., et al.: Revised gas-phase formation network of methyl cyanide: the origin of methyl cyanide and methanol abundance correlation in Hot Corinos. Mon. Not. R. Astron. Soc. **526**(3), 4535–4556 (2023)
30. Rosi, M., et al.: Electronic structure and kinetics calculations for the Si + SH reaction, a possible route of SiS formation regions. In: International Conference on Computational Science and Its Applications, pp. 306–315. Springer (2019)
31. Liang, P., et al.: OH ($^2\Pi$)+ C_2H_4 reaction: a combined crossed molecular beam and theoretical study. J. Phys. Chem. A **127**(21), 4609–4623 (2023)
32. Mancini, L., et al.: A computational characterization of the reaction mechanisms for the reactions n (^{2}D)+ CH_3CN and HC_3N and implications for the nitrogen-rich organic chemistry of titan. Comput. Theor. Chem. **1229**, 114341 (2023)
33. Mancini, L., et al.: Destruction of interstellar methyl cyanide (CH3CN) via collisions with HE+ ions. Astron. Astrophys. **691**, A83 (2024)
34. Richardson, V., et al.: Fragmentation of interstellar methanol by collisions with He^+: an experimental and computational study. Phys. Chem. Chem. Phys. **24**(37), 22437–22452 (2022)
35. Valença Ferreira de Aragão, E., Mancini, L., Faginas-Lago, N., Rosi, M., Skouteris, D., Pirani, F.: Semiempirical potential in kinetics calculations on the HC3N+ CN reaction. Mol. **27**(7), 2297 (2022)
36. Frisch, M., et al.: Fox: Gaussian 09, Revision A. 02, 2009, Gaussian. Inc., Wallingford CT (2009)

37. Werner, H.J., et al.: The Molpro quantum chemistry package. J. Chem. Phys. **152**(14), 144107 (2020)
38. Chai, J.D., Head-Gordon, M.: Systematic optimization of long-range corrected hybrid density functionals. J. Chem. Phys. **128**(8) (2008)
39. Dunning, Jr. T.H.: Gaussian basis sets for use in correlated molecular calculations. I. The atoms boron through neon and hydrogen. J. Chem. Phys. **90**(2), 1007–1023 (1989)
40. Kendall, R.A., Dunning, Jr. T.H., Harrison, R.J.: Electron affinities of the first-row atoms revisited. systematic basis sets and wave functions. J. Chem. Phys. **96**(9), 6796–6806 (1992)
41. Woon, D.E., Dunning, Jr. T.H.: Gaussian basis sets for use in correlated molecular calculations. III. The atoms aluminum through argon. J. Chem. Phys. **98**(2), 1358–1371 (1993)
42. Gonzalez, C., Schlegel, H.B.: An improved algorithm for reaction path following. J. Chem. Phys. **90**(4), 2154–2161 (1989). https://doi.org/10.1063/1.456010
43. Gonzalez, C., Schlegel, H.B.: Reaction path following in mass-weighted internal coordinates. J. Phys. Chem. **94**(14), 5523–5527 (1990). https://doi.org/10.1021/j100377a021
44. Bartlett, R.J.: Many-body perturbation theory and coupled cluster theory for electron correlation in molecules. Annu. Rev. Phys. Chem. **32**(1), 359–401 (1981)
45. Olsen, J., Jo/rgensen, P., Koch, H., Balkova, A., Bartlett, R.J.: Full configuration–interaction and state of the art correlation calculations on water in a valence double-zeta basis with polarization functions. J. Chem. Phys. **104**(20), 8007–8015 (1996)
46. Raghavachari, K., Trucks, G.W., Pople, J.A., Head-Gordon, M.: A fifth-order perturbation comparison of electron correlation theories. Chem. Phys. Lett. **157**(6), 479–483 (1989)
47. Martin, J.M.: Ab initio total atomization energies of small molecules–towards the basis set limit. Chem. Phys. Lett. **259**(5–6), 669–678 (1996)
48. Balucani, N., et al.: Combined crossed molecular beam and theoretical studies of the N(^{2}D)+ CH_4 reaction and implications for atmospheric models of titan. J. Phys. Chem. A **113**(42), 11138–11152 (2009). https://doi.org/10.1021/jp904302g
49. Skouteris, D., et al.: A theoretical investigation of the reaction H+SiS2 and implications for the chemistry of silicon in the interstellar medium. In: Gervasi, O., et al. (eds.) ICCSA 2018. LNCS, vol. 10961, pp. 719–729. Springer, Cham (2018). https://doi.org/10.1007/978-3-319-95165-2_50
50. Di Genova, G., et al.: Gas-phase formation routes of dimethyl sulfide in the interstellar medium. Astron. Astrophys. **704**, A305 (2025)
51. Lee, T.J., Taylor, P.R.: A diagnostic for determining the quality of single-reference electron correlation methods. Int. J. Quantum Chem. **36**(S23), 199–207 (1989)